JOURNAL OF PHYSICAL ORGANIC CHEMISTRY, VOL. 8, 597–604 (1995)

MONO-, BIS- AND TETRA-ACRIDINE LIGANDS: SYNTHESIS, X-RAY STRUCTURAL DETERMINATION AND DYNAMIC FLUORESCENCE MICROSCOPIC STUDIES ON THE MODIFICATION OF THE HIGHER ORDER STRUCTURE OF DNA

GRAHAM J. ATWELL AND WILLIAM A. DENNY

Cancer Research Laboratory, School of Medicine, The University of Auckland, Private Bag 92019, Auckland, New Zealand

GEORGE R. CLARK AND CHARMIAN J. O'CONNOR*

Department of Chemistry, The University of Auckland, Private Bag 92019, Auckland, New Zealand

AND

YUKIKO MATSUZAWA AND KENICHI YOSHIKAWA

Graduate School of Human Informatics, Nagoya University, Nagoya 464-01, Japan

A series of mono-, bis- and tetra-acridine ligands were prepared and their effects on the higher order structure of DNA were studied by dynamic fluorescence microscopy. The single-crystal structure of the bis-acridine derivative *N*-[2-(dimethylamino) ethyl]-4-[2-(9-acridinylamino)benzamido]-2-(9-acridinylamino)benzamide trihydrochloride (4) was determined, and shows that the molecule is sufficiently flexible to fold into an intramolecular stacking interaction in the crystal, supporting earlier hydrodynamic evidence that this compound can bis-intercalate into DNA forming a single base pair (bp) sandwich complex. The corresponding tetra-acridine analogue 1,11-bis[4-[2-(9-acridinylamino)benzamido]-2-(9-acridinylamino)phenyl]-1,11-dioxo-6-methyl-2,6,10-triazaundecane pentahydrochloride (6) was synthesized, and dynamic fluorescence microscopy was used to study the effects of 4 and 6 on the higher order structure of large T4 DNA molecules (166 kbp), by measuring the average long-axis length (persistence length, *l*) of the complexes. The mono-intercalating ligand acridine orange (5) increases *l*, whereas the bisintercalating diacridine 4 has no apparent effect and the putative multi-intercalating tetracridine derivative 6 decreases *l* by compacting the higher order DNA structure. These results demonstrate the usefulness of the technique for directly observing ligand–DNA complexes, and show that ligands with suitably positioned multiple binding sites can influence the higher order structure of DNA (and thus possibly gene expression).

INTRODUCTION

When two DNA-intercalating chromophores are linked by a flexible chain of minimum length, both chromophores can bind by intercalation (bis-intercalation). To be consistent with the 'excluded site' principle, which states that when an intercalator binds to a site in a DNA lattice, other intercalators are excluded from binding to the adjacent sites,[1] it has been assumed that bis-intercalation does not take place at contiguous sites, but at sites separated by a minimum of two base pairs (bp). However, this principle is only a thermodynamic postulate, and is not required by all models of intercalation.[2] Most work to date has been carried out with polymethylene- and alkylamide-linked diacridines (e.g. 1–3).[3–5]

This work shows that an abrupt change in binding mode occurs when the linker chain reaches a length of about 8.8 Å, with the unwinding angle increasing from ca 15° (mono-intercalation) to ca 30° (bis-intercalation). Compound **1** was postulated[3] to bind by bis-intercalation at contiguous sites, with one chromophore on either side of a single base pair, since the linking

* Author for correspondence.

CCC 0894–3230/95/090597–08

Received 2 May 1995
Accepted 30 May 1995

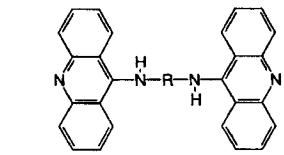

1. R=$(CH_2)_6$
2. R=$(CH_2)_nCONH(CH_2)_m$
3. R=$(CH_2)_2CONH(CH_2)_3NHCO(CH_2)_2$

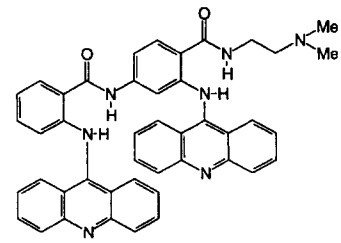

4.

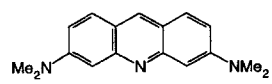

5.

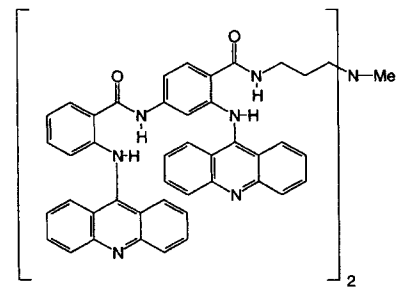

6.

chain is too short to span two base pairs if normal DNA geometry is maintained. However, this interpretation was not supported by later NMR studies,[6] which showed that **1** and related compounds bound to the self-complementary decadeoxynucleotide $d(AT)_5d(AT)_5$ by mono-intercalation only, suggesting that the binding mode is very condition dependent. Atwell et al.[7] then reported hydrodynamic data (an unwinding angle of 34°) for the more rigid diacridine **4**, suggesting that it also binds to DNA by bis-intercalation. Since model building indicated that the chromophores are rapidly held by the linker chain in a coplanar configuration only 7 Å apart, it was suggested that this compound must bind by bis-intercalation at contiguous sites. To study this postulate further, we have determined the crystal structure of **4**.

There have been extensive studies on the effects of intercalating ligands on both the local DNA structure close to the binding site (using x-ray crystallography and 2D NMR spectroscopy), and on higher order structures (mainly by electron microscopy; e.g. complexes with histone proteins[8]). However, the pretreatments necessary for the latter, including drying and metal deposition, which may well change the structure originally present in the aqueous environment, restrict the interpretation of these data in terms of the higher order structure of DNA. The technique also does not allow the observation of time-dependent structural changes.

It has recently been found[9,10] that dynamic information, including the effect of intercalating and minor groove binding ligands on the higher order structure of DNA, can be obtained by applying Yanagida et al.'s technique[11] for visualizing a single DNA molecule in an aqueous environment, using fluorescence microscopy and an appropriate fluorescent dye. One study[12] clearly showed that while a minor groove binder decreased the persistence length l of DNA (an index inversely proportional to the degree of bending of the DNA chain), but had no effect on the contour length, the intercalator ethidium bromide increased both the contour and the persistence length.[9,10] In this study, we used fluorescence microscopy to measure l for T4-DNA molecules (166 kbp) complexed with acridine orange (5) and with related bisacridine (4) and tetraacridine (6) derivatives.

EXPERIMENTAL

Preparation of N-[2-(dimethylamino)ethyl]-4-[2-(9-acridinylamino)benzamido]-2-(9-acridinylamino)benzamide trihydrochloride (**4**). A solution of 4-amino-2-nitrobenzoic acid (5·00 g, 27 mmol) in water (100 ml) containing Na_2CO_3 (4·37 g, 41 mmol) was treated in one portion with 2-nitrobenzoyl chloride (7·62 g, 41 mmol). The mixture was shaken at 20 °C for 0·5 h, then diluted with water (100 ml), neutralized with dilute AcOH, treated with charcoal and clarified by filtration. Acidification with dilute HCl provided a solid which was recrystallized twice from aqueous MeOH to give 4-(2-nitrobenzamido)2-nitrobenzoic acid (6·21 g, 68%), m.p. 229–231 °C. C, H, N Elemental analyses corresponded to $C_{14}H_9N_3O_7$. A stirred solution of this acid (3·31 g, 10 mmol) in DMF (15 ml) was treated with 1,1-carbonyldimidazole (1·95 g, 12 mmol) at 20 °C, then cooled to 0 °C and treated with N,N-dimethylethylenediamine (1·32 g, 15 mmol). The mixture was allowed to warm to 20 °C and then diluted with aqueous Na_2CO_3. The resulting solid was crystallized from aqueous EtOH then from EtOH to give N-[2-(dimethylamino)ethyl]4-(2-nitrobenzamido)-2-nitrobenzamide (71%), m.p. 192–193 °C. C, H, N Elemental analyses corresponded to $C_8H_{19}N_5O_6$. A solution of the above amide (2·01 g, 5·0 mmol) in MeOH was hydrogenated over 5% Pd/C at 60 psi for 3 h. The catalyst was removed and the solution was evaporated to dryness under reduced pressure. The resulting solid was dissolved in dry N-methylpyrrolidone at 20 °C and treated with a 9-chloroacridine (2·14 g, 10·0 mmol) followed by concentrated HCl (0·47 ml, 5·5 mmol). The solution was stirred and heated at 50 °C for 15 min, then diluted with excess EtOAc. The precipitated solid was recrystallized twice from MeOH–EtOAc to give N-[2-(dimethylamino)ethyl]-4-[2-(9-(acridinylamino)benzamido]-2-(9-acridinylamino)benzamide trihydrochloride (4) (72%), m.p. 252–253 °C. C, H, N, Cl Elementary analyses corresponded to $C_{44}H_{37}N_7O_2 \cdot 3HCl$.

Preparation of 1,11-bis[4-[2-(9-acridinylamino)benzamido]-2-(9-acridinylamino)phenyl]-1,11-dioxo-6-methyl-2,6,10-triazaundecane pentahydrochloride (**6**). A stirred solution of 4-nitrophenol (1·60 g, 11·5 mmol) in pyridine (10 ml) was treated dropwise at 5 °Cwith PCl_3 (0·52 g, 3·8 mmol) and the mixture was then stirred at 20 °C until conversion into a uniform white precipitate was achieved. 4-(2-Nitrobenzamido)-2-nitrobenzoic acid (2·00 g, 6·0 mmol) was then added and the mixture was stirred at 20 °C until homogeneous and then reheated under reflux for 10 min. Concentration under reduced pressure followed by dissolution of the residue in Me_2CO and dilution with water provided a crystalline solid, which was washed with water and benzene to give 4-nitrophenol 4-(2-nitrobenzamide)-2-nitrobenzoate (2·20 g, 81%), which was employed without further purification. A stirred solution of the preceding ester (1·00 g, 2·2 mmol) in DMF (3 ml) was treated at 5 °C with NEt_3 (0·23 g, 2·3 mmol) followed by 5-methyl-1,5,9-triazanonane (0·16 g, 1·1 mmol). The mixture was stirred at 20 °C for 1 h, then diluted with water. The resulting solid was collected and recrystallized three times from DMF–EtOH to give 1,11-bis[4-(2-nitrobenzamido)-2-nitrophenyl]-1,11-dioxo-6-methyl-2,6,10-triazaundecane (0·67 g, 79%), m.p. 227–228 °C. C, H, N Elementary analyses corresponded to $C_{35}H_{33}N_9O_{12}$. The above compound (0·50 g, 0·77 mmol) was dissolved in MeOH (50 ml) containing 1 M HCl (0·7 ml) and hydrogenated over 5% Pd/C at 60 psi for 5 h. The catalyst was removed and the solution was evaporated to dryness under reduced pressure. A suspension of the resulting solid in N-methylpyrrolidone (4 ml) and MeOH (4 ml) was treated with 9-chloracridine (0·65 g, 3·04 mmol) followed by concentrated HCl (1 drop), and the mixture was stirred at 20 °C for 1 h. Dilution with EtOAc provided a solid which was recrystallized three times from MeOH–EtOAc (removing insoluble impurities by filtration) to give 1,11-bis[4-[2-(9-acridinylamino)benzamido]-2-(9-acridinylamino)phenyl]-1,11-dioxo-6-methyl-2,6,10-triazaundecane pentahydrochloride (6) (69%), m.p. 253–256 °C. C, H, N, Cl Elemental analyses corresponded to $C_{87}H_{69}N_{13}O_4 \cdot 5HCl \cdot H_2O$.

X-ray crystallography. Unit cell dimensions were obtained from a least-squares fit to the four-circle coordinates of 25 reflections recorded on a Nonius CAD-4 diffractometer. Data collection employed $\omega/2\theta$ scans using graphite monochromated Mo Kα radiation. The scan angle was $0{\cdot}8 + 0{\cdot}345 \tan\theta$ and reflections were counted until $\sigma(I)/I$ was 0·02 or for a maximum of 45 s. Three reflections monitored throughout data collection as a check on crystal movement or decomposition showed a steady decline to 94% of their initial values. Data were scaled accordingly, and corrected for Lorentz and polarization effects and for absorption using empirical psi scans.[13] The structure was solved by direct methods[14] and refinement was by full-matrix least-squares.[15] Scattering factors were taken from *International Tables for X-Ray Crystallography*[16] and were for neutral atoms. Hydrogen atoms were placed in calculated positions, with methyl hydrogens being treated as rigid groups. The difference electron density map showed that the crystals contain molecules of acetone of crystallization. Full details of crystal data and refinement parameters are given in Table 1. The crystals contain one molecule of compound per crystallographic asymmetric unit, along with a disordered acetone molecule of solvation. Atomic coordinates are

Table 1. Crystal data for **4**

Formula	$C_{44}H_{40}Cl_3N_7O_2 \cdot 0{\cdot}5C_3H_6O$
Molecular weight	805·21
Crystal system	Triclinic
Space group	$P-1$
a	8·501(3) Å
b	13·841(4) Å
c	17·900(13) Å
α	81·56(3)°
β	82·25(4)°
γ	73·00(2)°
V	1982·8(16) Å^3
Z	2
d(calc.)	1·41 g cm^{-3}
μ	2·88 cm^{-1}
X-rays Mo Kα (monochromatic)	$\lambda = 0{\cdot}71069$ Å
Temperature	−100 °C
Diffractometer	Nonius CAD4
Scan technique	$\omega/2\theta$
2θ (min.–max.)	2–46°
No. of unique reflections	3360, $R_{int} = 0{\cdot}069$
No. of observed reflections	1583 [$I > 2{\cdot}5\sigma(I)$]
Crystal size	0·31 × 0·23 × 0·04 mm
Crystal colour and habit	Yellow–orange, platelets
A (min.–max.)	0·996–0·915
Least-squares weights	$3{\cdot}324/[\sigma(F^2) + 0{\cdot}00154F^2]$
Function minimized	$\Sigma w[\lvert F_o \rvert - \lvert F_c \rvert]^2$
R and R'	0·108, 0·108

listed in Table 2. The molecular geometry and atomic numbering are depicted in Figures 1 and 2. Supplementary data consisting of thermal parameters, hydrogen coordinates, full listings of bond lengths and angles and structure factor tables are available from the authors (G.R.C.).

Dynamic fluorescence microscopy. The ligands were dissolved in TBE buffer (45 mM Tris–45 mM borate–1 mM EDTA) containing T4-DNA. The samples were allowed to stand for 10 min, then 4',6-diamidino-2-phenylindole (DAPI) and 2-mercaptoethanol were added, to give the final concentrations noted in Figure 3. It has been confirmed[10] that DAPI shows a negligible effect on both the contour length and the persistence length under the experimental conditions employed in this study. Ligand/DNA nucleotide ratios were varied from 0·1 to 10. The complexes were viewed with a Cole Zeiss Axiovert 135 TV microscope equipped with a 100× oil-immersed objective lens, and illuminated with 365 nm UV radiation. The fluorescence images were recorded on video tapes using a high-sensitivity SIT TV camera and an Argus 10 (Hamamatsu Photonics) image processor.

Table 2. Atomic coordinates for **4**

Atom	x	y	z	U_{iso}
C11	0·1436(7)	0·5557(4)	0·1685(3)	0·044(4)
C12	0·3084(7)	0·4273(5)	0·4625(4)	0·072(5)
C13	0·476(2)	0·4166(12)	0·6195(14)	0·373(25)
O1	0·9502(17)	0·1887(9)	−0·1761(8)	0·032(10)
O2	1·4209(15)	−0·0802(9)	0·1703(8)	0·029(9)
N1	1·034(2)	0·3386(11)	−0·3096(10)	0·036(12)
N2	1·2248(19)	0·1479(10)	−0·2060(9)	0·023(11)
N3	0·847(2)	0·2353(11)	−0·0358(10)	0·030(12)
N4	0·453(2)	0·4148(11)	0·0891(10)	0·032(12)
N5	1·1535(19)	0·0167(10)	0·1582(9)	0·023(11)
N6	0·950(2)	0·0476(11)	0·2834(10)	0·039(12)
N7	0·595(2)	0·2954(11)	0·3570(11)	0·036(13)
C1	1·037(2)	0·4408(15)	−0·3539(13)	0·042(7)
C2	0·893(3)	0·3100(18)	−0·3358(14)	0·056(7)
C3	1·194(2)	0·2630(14)	−0·3269(12)	0·034(6)
C4	1·210(2)	0·1570(13)	−0·2853(11)	0·026(5)
C5	1·090(2)	0·1571(15)	−0·1527(12)	0·025(5)
C6	1·118(2)	0·1241(14)	−0·0727(11)	0·019(5)
C7	1·260(2)	0·0534(13)	−0·0502(12)	0·025(5)
C8	1·278(2)	0·0166(14)	0·0241(11)	0·019(5)
C9	1·155(2)	0·0489(14)	0·0796(12)	0·022(5)
C10	1·010(2)	0·1211(13)	0·0590(11)	0·021(5)
C11	0·995(2)	0·1611(14)	−0·0127(11)	0·021(5)
C12	0·720(2)	0·2972(14)	0·0052(12)	0·022(5)
C13	0·744(2)	0·3395(14)	0·0694(12)	0·022(5)
C14	0·894(2)	0·3389(14)	0·0963(12)	0·029(6)
C15	0·909(2)	0·3809(13)	0·1581(11)	0·024(5)
C16	0·759(2)	0·4299(15)	0·1981(13)	0·038(6)
C17	0·609(2)	0·4387(14)	0·1791(11)	0·028(6)
C18	0·612(2)	0·3974(15)	0·1150(12)	0·026(6)
C19	0·427(2)	0·3828(15)	0·0256(13)	0·026(6)
C20	0·265(2)	0·4046(15)	0·0029(12)	0·032(6)
C21	0·241(3)	0·3699(16)	−0·0601(13)	0·047(7)
C22	0·376(2)	0·3091(15)	−0·1025(13)	0·039(6)
C23	0·531(2)	0·2844(15)	−0·0843(12)	0·037(6)
C24	0·557(2)	0·3217(15)	−0·0189(12)	0·031(6)
C25	1·274(2)	−0·0430(15)	0·2005(12)	0·026(5)
C26	1·232(2)	−0·0630(14)	0·2817(12)	0·024(5)
C27	1·349(2)	−0·1371(15)	0·3237(12)	0·034(6)
C28	1·321(2)	−0·1624(15)	0·4006(12)	0·028(5)
C29	1·164(2)	−0·1116(15)	0·4373(13)	0·033(6)
C30	1·048(2)	−0·0420(13)	0·4005(11)	0·018(5)
C31	1·080(2)	−0·0160(15)	0·3235(12)	0·025(5)
C32	0·851(2)	0·1359(14)	0·3061(11)	0·022(5)
C33	0·877(2)	0·2024(15)	0·3518(12)	0·031(6)
C34	1·039(2)	0·1953(15)	0·3669(12)	0·034(6)
C35	1·069(2)	0·2582(15)	0·4138(12)	0·039(6)
C36	0·933(2)	0·3313(15)	0·4419(12)	0·039(6)
C37	0·781(2)	0·3415(16)	0·4275(12)	0·040(6)
C38	0·749(2)	0·2802(16)	0·3766(12)	0·031(6)
C39	0·561(2)	0·2472(16)	0·3006(12)	0·027(5)
C40	0·403(2)	0·2773(16)	0·2769(12)	0·034(6)
C41	0·374(2)	0·2326(16)	0·2201(12)	0·038(6)
C42	0·492(2)	0·1517(15)	0·1863(13)	0·038(6)
C43	0·640(2)	0·1230(15)	0·2140(12)	0·032(6)
C44	0·690(2)	0·1664(16)	0·2715(13)	0·033(6)
O3	0·6800(0)	−0·0936(0)	0·4542(0)	0·1000(0)
C45	0·5400(0)	−0·0800(0)	0·5600(0)	0·1000(0)
C46	0·5700(0)	−0·0400(0)	0·4900(0)	0·1000(0)
C47	0·5000(0)	0·0400(0)	0·4300(0)	0·1000(0)

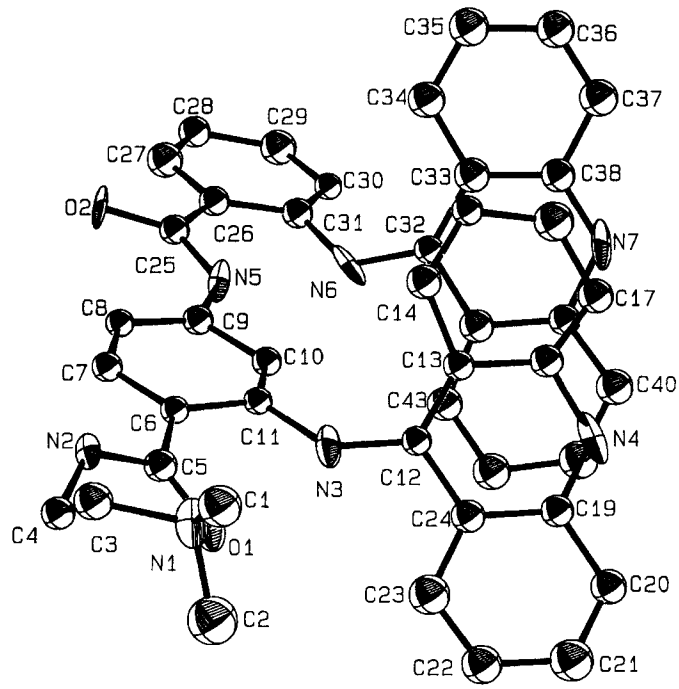

Figure 1. Molecular geometry and atomic numbering of **4**. Atoms are represented as 50% probability surfaces

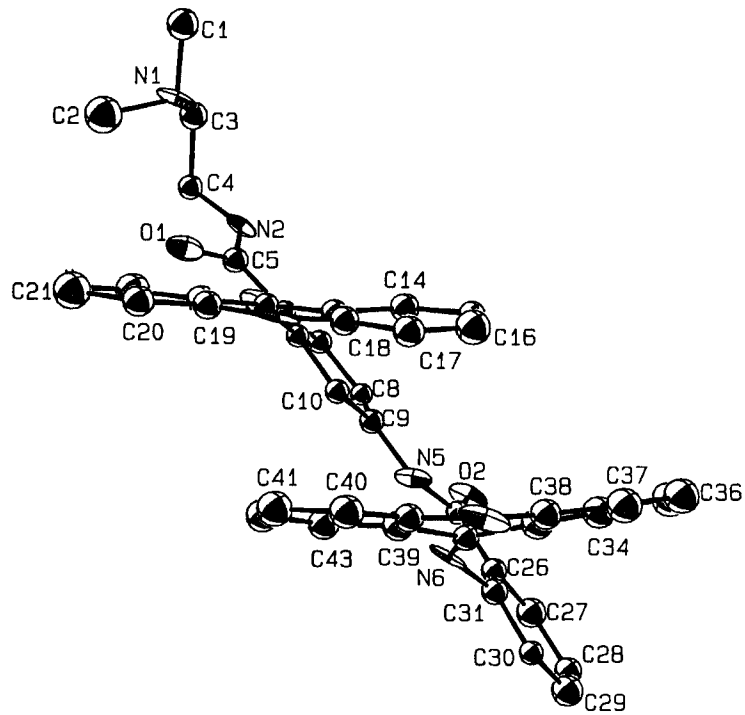

Figure 2. Side-on view of the intramolecular acridine stacking in **4**

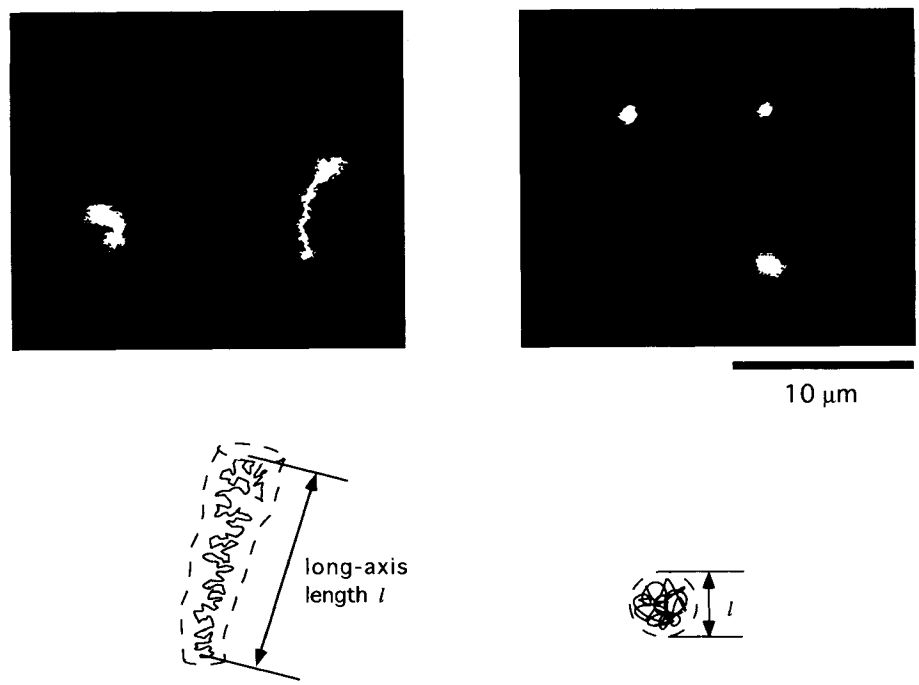

Figure 3. Freeze frame of fluorescence microscopic picture of T4-DNA molecules bound to **4** (left-hand side) and **6** (right-hand side) at [drug]/[nucleotide] = 5. Scale bar indicates 10 μm. Conditions: T4-DNA (166 kbp) and drug (**5**, **4** or **6**) were added to TBE buffer (45 mM Tris–45 μM borate–1 mM EDTA), allowed to stand for 10 min and then the fluorescent dye DAPI and the antioxidant 2-mercaptoethanol were added.[12,16] Final concentrations: DNA in nucleotide, 0·6 μM; DAPI, 0·6 μM; 2-mercaptoethanol, 4% (v/v); the [drug]/[nucleotide] ratios were varied from 0·1 to 10. The resolution limit was *ca* 0·2 nm

RESULTS AND DISCUSSION

It has been shown previously[7] that the bisacridine **4** is a bis-intercalator, probably at contiguous sites on DNA, with model-building indicating a possible conformation where the chromophores are in a coplanar configuration only 7 Å apart. The crystal structure of **4** showed all bonds and angles to be normal, but both acridine rings are significantly non-planar. The ring defined by atoms N(4), C(12)–C(24) is distorted in the region C(14)–C(16), while the ring defined by atoms N(7), C(32)–C(44) is considerably more distorted by buckles at N(7) and C(32) and a bend through the central N(7)–C(32) axis, with the overall effect being that of a 'butterfly' geometry (Figures 1 and 2).

The molecule undergoes an intramolecular stacking interaction involving two rings of each acridine. The closest approaches are C(17)–C(39) 3·26 Å and N(4)–C(41) 3·34 Å, with five others closer than 3·6 Å. The three chloride ions make different contacts with the protonated sites on the molecule. Cl(1) has a strong interaction (approach distances 3·09 Å) with both N(4) and N(1) in different molecules. Cl(2) makes a single approach (3·16 Å) to N(7), but Cl(3) is not close to any N atoms, merely occupying an interstice in the crystal lattice. This may explain the poor resolution of Cl(3) in the electron density maps and its high thermal parameters in the least-squares refinement.

The crystal structure shows that **4** is sufficiently flexible to allow the two acridine moieties to stack (in the solid state); its geometry is not restricted to the extended conformation observed in bis-intercalators containing more flexible linker chains. Model construction shows that it is possible for the acridine ring systems to move apart to a maximum separation distance of approximately 7·5 Å, within the range required for bis-intercalation at contiguous sites on DNA, providing support for the original postulate[7] that **4** could act as a DNA bis-intercalator at contiguous sites. Studies of **4** complexed to oligonucleotides are in progress.

The ability of **4** to bind to DNA in this fashion prompted us to prepare the corresponding tetra-acridine **6**, where two sets of such 'contiguous' binding sites are available. It has been shown recently that compounds of this general type, with acridine intercalators joined by rigid linker chains in a pre-organized geometry, can

affect higher order DNA structure by 'intermolecular bisintercalation' between distance linear sections of the same molecule which are close in space. Mullins et al.[17] demonstrated that such interactions occur with diacridine **7**, using a DNA ligation technique to generate catenanes from DNA molecules cross-linked temporarily by intermolecular bisintercation.

Hydrodynamic assays were not able to distinguish the degree of interaction of **6** with DNA (data not shown). However, using dynamic fluorescence microscopy we were able to demonstrate that **6** and the mono-intercalator acridine orange (**5**) induce opposite effects on the higher order structure of DNA. Figure 3 shows typical freeze frames (converted to black and white pictures) for T4-DNA molecules complexed with **4** and **6** (ligand/nucleotide ratio 5), from which the time-averaged long-axis length (persistence length l) of the complex can be determined. Complexes obtained with **4** had a string-like appearance (large l) and low fluorescence intensity, but the complexes with **6** were condensed into globules (small l) and had much greater fluorescence intensity. Figure 4 shows the dependence on l on the ligand/nucleotide ratio for compounds **4–6**. With increasing concentrations of the mono-intercalator **5**, l increases linearly. Surprisingly, the putative bisintercalator **4** showed a lesser effect, although this compound has been shown to extend the DNA contour length in hydrodynamic assays.[7] However, the tetra-acridine **6** induces dramatic compaction of the DNA, with a critical ligand/nucleotide ratio of about 2.

It has been reported[10] that, under buffer conditions similar to those employed here, the contour length (L) of T4-DNA is 57 mm and the persistence length (l) is 60 nm. This indicates that the conformation of T4 is adequately described by the random-flight model,[18] and comprises about 1000 (L/l) rigid segments of length l connected by freely-movable joints. On addition of a monointercalator such as **5**, both L and l increase, extending the observed time-averaged length l of the complex.[19] While the bisacridine **4** must also similarly increase L and l by local intercalation, this may be offset by through-space electrostatic interactions of the flexible cationic side-chain with sequentially distant DNA segments. When this cationic charge is replaced, in the tetracridine **6**, by another bis-intercalating unit, the resulting through-space interactions result in compaction of the DNA. A similar explanation has been put forward[19] to explain the formation of catenanes by ligation following the temporary cross-linking of remote DNA segments by a series of rigidly linked diacridines such as **7**.

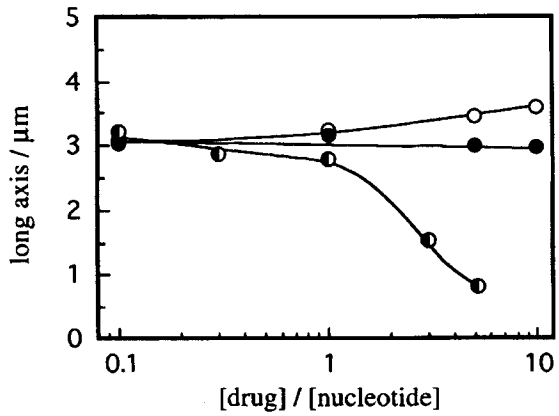

Figure 4. Concentration dependence of the persistence length (*l*) of T4-DNA molecules bound to (O) **5**, (●) **4** and (O) **6** under the conditions described in Figure 3

CONCLUSIONS

These results show the usefulness of dynamic fluorescence microscopy as a technique for directly observing the physical consequences of the interaction of intercalating ligands with large DNA molecules. They confirm work by others[19,20] that complexing by mono-intercalators prevents or destroys condensation of DNA to the compact form, and show that it may be possible to control the higher order structure of DNA by complexing with ligands possessing multiple binding sites. Such changes in higher order DNA structure are important in the regulation of gene expression by the cooperative binding of proteins. The demonstration that **6** induces the formation of condensed DNA with a distribution of sizes and possible conformations (data not shown) similar to those induced by DNA-binding proteins[21] suggests that small molecule control of gene expression through alteration of high-order structure may be possible with appropriate small molecules.

ACKNOWLEDGEMENTS

This study was partly supported by a Grant-in-Aid for Scientific Research from the Ministry of Education, Science and Culture of Japan and by the Auckland Division of the Cancer Society of New Zealand.

REFERENCES

1. P. H. von Hippel and J. D. McGhee, *J. Mol. Biol.* **86**, 469–489 (1974).
2. R. H. Schafer and M. J. Waring, *Biopolymers* **21**, 2279–2290 (1982).
3. L. P. G. Wakelin, M. Romanos, T. K. Chen, D. Glaubiger, E. S. Canellakis and M. J. Waring, *Biochemistry* **17**, 5057–5063 (1978).
4. H. D. King, W. D. Wilson and E. J. Gabbay, *Biochemistry* **21**, 4982–4989 (1982).
5. W. A. Denny, G. J. Atwell, B. C. Baguley and L. P. G. Wakelin, *J. Med. Chem.* **28**, 1568–1574 (1985).

6. N. Assa-Munt, W. A. Denny, W. Leupin and D. R. Kearns, *Biochemistry* **24**, 1441–1449 (1985).
7. G. J. Atwell, G. M. Stewart, W. Leupin and W. A. Denny, *J. Am. Chem. Soc.* **107**, 4335–4336 (1985).
8. A. L. Olins and D. E. Olins, *Science* **183**, 330–332 (1974).
9. M. Matsumoto, T. Sakaguchi, T. Kimura, M. Doi, K. Minagawa, Y. Matsuzawa and K. Yoshikawa, *J. Polym. Sci. B* **30**, 779–783 (1992).
10. Y. Matsuzawa and K. Yoshikawa, *Nucleosides Nucleotides* **13**, 1415–1423 (1994).
11. M. Yanagida, Y. Hiraoka and I. Katsura, *Cold Spring Harbor Symp. Quant. Biol.* **47**, 177–187 (1983).
12. Y. Masubuchi, H. Oana, K. Ono, M. Matsumoto, M. Doi, K. Minigawa, Y. Matsuzawa and K. Yoshikawa, *Macromolecules* **26**, 5269–5270 (1993).
13. A. C. North, D. C. Phillips and F. S. Mathews, *Acta Crystallogr., Sect. A* **24**, 351–359.
14. G. M. Sheldrick, *Acta Crystallogr., Sect. A* **46**, 467–473 (1990).
15. G. M. Sheldrick, *SHELX-76. Program for Crystal Structure Determination.* University of Cambridge, Cambridge (1976).
16. *International Tables for X-Ray Crystallography*, Vol. IV. Kynoch Press, Birmingham (1974).
17. S. T. Mullins, N. K. Annan, P. R. Cook and G. Lowe, *Biochemistry* **31**, 842–849 (1992).
18. W. A. Denny and L. P. G. Wakelin, *Anti-Cancer Drug Des.* **2**, 71–77 (1987).
19. K. G. Krishna, T. K. S. Kumar and M. W. Pandit, *Biopolymers* **33**, 1415–1420 (1993).
20. S.-M. Cheng and S. C. Mora, *Biopolymers* **14**, 663–674 (1975).
21. K. Minagawa, Y. Matsuzawa, K. Yoshikawa, M. Matsumoto and M. Doi, *FEBS Lett.* **296**, 67–69 (1991).